Spontaneous Generation of Stable Pnictinyl Radicals from "Jack-in-the-Box" Dipnictines: A Solid-State, Gas-Phase, and Theoretical Investigation of the Origins of Steric Stabilization[1]

Sarah L. Hinchley,[†] Carole A. Morrison,[†] David W. H. Rankin,*[,†] Charles L. B. Macdonald,[‡] Robert J. Wiacek,[‡] Andreas Voigt,[‡] Alan H. Cowley,*[,‡] Michael F. Lappert,*[,⊥] Grete Gundersen,[||] Jason A. C. Clyburne,[§] and Philip P. Power[#]

Contribution from the Department of Chemistry, University of Edinburgh, West Mains Road, Edinburgh, EH9 3JJ, Scotland, Department of Chemistry and Biochemistry, The University of Texas at Austin, Austin, Texas 78712, School of Chemistry, Physics and Environmental Sciences, University of Sussex, Falmer, Brighton BN1 9RH, England, Department of Chemistry, University of Oslo, Box 1033, Blindern, N-0315 Oslo, Norway, Department of Chemistry, Acadia University, Wolfville, NS B0P 1X0, Canada, and Department of Chemistry, The University of California, Davis, Davis, California 95616

Received March 7, 2001

Abstract: The molecular structures of the stable phosphinyl and arsinyl radicals, $^{\bullet}PnR_2$ [Pn = P (**2**); As (**4**); R = $CH(SiMe_3)_2$], have been determined by gas-phase electron diffraction (GED) in conjunction with ab initio molecular orbital calculations. The X-ray crystal structures of the corresponding dipnictines, the "dimers", R_2PnPnR_2 [Pn = P (**1**), As (**3**)], and the chloro derivatives R_2PnCl [Pn = P (**5**), As (**6**)] have also been determined. Collectively, these structural investigations demonstrate that large distortions of the ligands attached to Pn occur when the pnictinyl radicals unite to form the corresponding dipnictine dimers. Principally, it is the shape and flexibility of the $CH(SiMe_3)_2$ ligands that permit the formation of the P−P and As−As bonds in **1** and **3**, respectively. However, theoretical studies indicate that in the process of pnictinyl radical dimerization to form **1** and **3**, both molecules accumulate substantial amounts of potential energy and are thus primed to spring apart upon release from the solid state by melting, dissolution, or evaporation. The insights gleaned from these unusual systems have permitted a deeper understanding of the functioning of sterically demanding substituents.

Introduction

The use of bulky ligands to stabilize compounds that are otherwise too reactive to be isolated is one of the major developments in modern chemistry. By means of such stabilization (both kinetic and in some cases, including this one, also thermodynamic), it has proved possible to isolate, characterize, and study a number of intriguing species that include coordinatively unsaturated neutral molecules (carbene analogues),[2] cations,[3] and radicals[4,5] as well as a host of novel multiply bonded derivatives.[6] However, not withstanding the importance and ubiquity of sterically demanding ligands, there have been few studies regarding the origins and nature of the stabilization afforded by them. The particular focus of the present work is to probe the factors that underlie the stabilization of phosphinyl ($^{\bullet}PR_2$) and arsinyl ($^{\bullet}AsR_2$) radicals. By way of background, it is worth recalling that, despite the important of e.g. nitroxides as contrast enhancing agents for magnetic resonance imaging (MRI) and as probes for EPR imaging,[7] surprisingly few neutral radicals featuring main group elements have actually been isolated.

In general, the homolytic cleavage of the E−E single bonds of molecules of the general type $R'_nEER'_n$ and the consequent formation of the corresponding $R'_nE^{\bullet}$ radicals or neutral molecules is expected to be favored by increased steric bulk of the ligands R′. The conventional view is that such increases of steric strain would be manifested primarily in elongation of the E−E bond and that beyond a critical point of steric loading this bond would rupture. Our preliminary work[1] has suggested that the conventional view is oversimplified. An X-ray analysis of the bulky diphosphine R_2PPR_2 [**1**; R = $CH(SiMe_3)_2$] revealed that, in fact, the potential energy of steric repulsion is not manifested in an unduly elongated P−P bond. Moreover, a gas-phase electron diffraction (GED) study of the companion radical $^{\bullet}PR_2$ (**2**) showed that a conformational change from *syn,syn* to *syn,anti* is necessary before dimerization can occur. As a consequence of this conformational change, diphosphine **1** accumulates a considerable amount of potential energy due to a plethora of distortions of the $CH(SiMe_3)_2$ ligands. Collectively, these distortions constitute an energy storage reservoir, hence **1** is primed to spring apart upon dissolution, melting, or evaporation.

In a present paper we furnish full details of the experimental and theoretical work on the phosphorus system. However, to establish more generality for our preliminary conclusions, we also report new results for the analogous arsenicals R_2AsAsR_2

[†] University of Edinburgh.
[‡] The University of Texas at Austin.
[⊥] University of Sussex.
[||] University of Oslo.
[§] Acadia University.
[#] The University of California.

(1) For a preliminary account of the phosphinyl radical/diphosphine system, see: Hinchley, S. L.; Morrison, C. A.; Rankin, D. W. H.; Macdonald, C. L. B.; Wiacek, R. J.; Cowley, A. H.; Lappert, M. F.; Gundersen, G.; Clyburne, J. A. C.; Power, P. P. *Chem. Commun.* **2000**, 2045.

10.1021/ja010615b CCC: $20.00
Published on Web 08/22/2001

Table 1. Summary of X-ray Crystallographic Data for R_4P_2 (**1**), R_4As_2 (**3**), R_2PCl (**5**), and R_2AsCl (**6**); R = $CH(SiMe_3)_2$

	1	**3**	**5**	**6**
empirical formula	$C_{28}H_{76}P_2Si_8$	$C_{28}H_{76}As_2Si_8$	$C_{14}H_{38}ClPSi_4$	$C_{14}H_{38}AsClSi_4$
formula weight	699.54	784.44	385.22	429.17
temperature (K)	183(2)	153(2)	153(2)	183(2)
wavelength (Å)	0.71073	0.71073	0.71073	0.71073
crystal system	monoclinic	triclinic	monoclinic	monoclinic
space group	$P2_1/c$	$P\bar{1}$	$P2_1/n$	$P2_1/n$
unit cell dimensions:				
a (Å)	18.341(2)	20.348(4)	9.3297(2)	11.5626(11)
b (Å)	13.4240(10)	26.342(5)	12.3617(3)	12.3944(10)
c (Å)	19.033(2)	37.012(7)	20.4170(5)	17.542(2)
α (deg)	90	102.11(3)	90	90
β (deg)	110.650(10)	104.54(3)	95.174(1)	108.276(9)
γ (deg)	90	102.35(3)	90	90
volume (Å^3)	4385.0(7)	18015(6)	2345.2(1)	2387.2(4)
Z	4	16	4	4
density (calcd) (g cm^{-3})	1.060	1.161	1.091	1.194
absorption coeff. (cm^{-1})	3.35	17.13	4.29	17.30
F(000)	1544	6752	840	912
θ range for data collection (deg)	1.19 to 25.06	2.92 to 27.47	2.99 to 30.49	1.87 to 30.00
limiting indices	$-20 < h < 21$, $-2 < k < 15$, $-22 < l < 21$	$-6 < h < 6$, $-34 < k < 9$, $-42 < l < 48$	$-12 < h < 12$, $-17 < k < 16$, $-20 < l < 28$	$-1 < h < 16$, $-1 < k < 17$, $-24 < l < 23$
no. of reflcns collected	9263	100000	22517	8258
no. of independent reflcns	7709	27687	6325	6795
R_{int}	0.0173	0.0614	0.0476	0.0905
absorption correction	integration	none	none	none
data/restraints/parameters	7702/0/360	27654/0/2737	6325/0/201	6793/0/182
goodness-of-fit on F^2	1.705	1.511	1.034	1.043
final R indices [$I > 2\sigma(I)$]	$R1 = 0.0375$, $wR2 = 0.1159$	$R1 = 0.0531$, $wR2 = 0.1213$	$R1 = 0.0427$, $wR2 = 0.0971$	$R1 = 0.0582$, $wR2 = 0.1377$
R indices (all data)	$R1 = 0.0451$, $wR2 = 0.1203$	$R1 = 0.0913$, $wR2 = 0.1344$	$R1 = 0.0798$, $wR2 = 0.0906$	$R1 = 0.0897$, $wR2 = 0.1567$
largest diff. peak and hole (e Å^{-3})	0.295 and 0.312	0.536 and 0.522	0.417 and 0.310	1.831 and 0.879

(**3**) and $^{\bullet}AsR_2$ (**4**). Specifically, in view of the larger covalent radius of arsenic, we were curious whether the same conclusions regarding conformational changes, ligand flexibility, and potential energy storage would still obtain. Further generality for these ideas is evident from the structures of the closely related neutral group 14 species, MR_2 (M = Ge, Sn) and their cognate dimers.[8,9] In the solid state the conformation of each MR_2 moiety in the M_2R_4 dimer approximates to *syn,anti* but in gaseous MR_2 it approximates to *syn,syn*.

Previous EPR spectroscopic experiments on solutions of radicals **2** and **4** in toluene showed that each is indefinitely stable at 300 K.[4] On the basis of coupling constants, it was concluded that they are π-radicals[4] with the odd electron predominantly in a valence p-orbital. The stability of these radicals in the gas phase and solution is a further noteworthy feature.

Experimental Section

General Methods. All manipulations were carried out with the strict exclusion of air and moisture by handling materials under vacuum or in an atmosphere of dry argon. The chloropnictines, R_2PnCl {Pn = P (**5**), As (**6**); R = $[CH(SiMe_3)_2]$}, were synthesized as described in the literature.[4] Compounds **1** and **3** were prepared according to methods described previously[4] or by slight variations theoreof[10] (see the next section). Comprehensive details of the single-crystal X-ray diffraction and GED experiments are provided in the Supporting Information.

Crystallization and X-ray Diffraction Studies. Crystalline samples of **5** and **6** suitable for X-ray diffraction study were obtained by slow cooling of concentrated CH_2Cl_2 solutions of these compounds to 253 K. Crystals of diphosphine **1**, in an admixture with those of the starting chlorophosphine **5**, were obtained by slow cooling (to 279 K) of the red solution obtained from the sodium metal reduction of **5** in hexanes.[10] The yellow crystals of **1** and colorless crystals of **5** were separated manually with the aid of a microscope. Diarsine **3** was prepared by treatment of a pentane solution of R_2AsI (obtained via the reaction of Me_3SiI with **6**) with Li metal. Following filtration of the reaction mixture, concentration of the resulting orange solution afforded crystals of **3**. Yellow crystals of **3** suitable for X-ray analysis were obtained by slow cooling of the hexane solution to 253 K.

A summary of crystallographic data for **1**, **3**, **5**, and **6** is presented in Table 1 and complete details are provided in the Supporting Information.

Gas-Phase Electron Diffraction (GED) Studies. A detailed description of the GED experimental and data collection procedures is provided in the Supporting Information. The structures of **2** and **4** were

(2) For silylenes, see e.g.: Haaf, M.; Schmedake, T. A.; West, R. *Acc. Chem. Res.* **2000**, *33*, 704. Gehrhus, B.; Lappert, M. F. *J. Organomet. Chem.* **2001**, *617/618*, 209.

(3) For phosphenium and arsenium cations, see e.g.: Cowley, A. H.; Kemp, R. A. *Chem. Rev.* **1985**, *85*, 367. Carmalt, C. J.; Lomelí, V.; McBurnett, B. G.; Cowley, A. H. *Chem. Commun.* **1997**, 2095.

(4) (a) Gynane, M. J. S.; Hudson, A.; Lappert, M. F.; Power, P. P.; Goldwhite, H. *J. Chem. Soc., Chem. Commun*. **1976**, 623. (b) Gynane, M. J. S.; Hudson, A.; Lappert, M. F.; Power, P. P.; Goldwhite, H. *J. Chem. Soc., Dalton Trans*. **1980**, 2428.

(5) For very recent work on stable phosphorus radicals, see: Loss, S.; Magistrato, A.; Lataldo, L.; Hoffmann, S.; Geoffrey, M.; Rothlisberger, U.; Grützmacher, H. *Angew. Chem., Int. Ed. Engl.* **2001**, *40*, 723.

(6) Power, P. P. *Chem. Rev.* **1999**, *99*, 3463.

(7) See, for example: (a) Keana, J. F. W.; Lex, L.; Mann, J. S.; May, J. M.; Park, J. H.; Pou, S.; Prabhu, V. S.; Rosen, G. M.; Sweetman, B. J.; Wu, Y. *Pure Appl. Chem.* **1990**, *62*, 201. (b) Sotgiu, A.; Placidi, G.; Gualtieri, G.; Tatone, C.; Campanella, C. *Magn. Reson. Chem.* **1995**, *33*, 5160 and references therein.

(8) (a) Fjeldberg, T.; Haaland, A.; Schilling, B. E. R.; Lappert, M. F.; Thorne, A. J. *J. Chem. Soc., Dalton Trans.* **1986**, 1551. (b) Goldberg, D. E.; Hitchcock, P. B.; Lappert, M. F.; Thomas, K. M.; Thorne, A. J.; Fjeldberg, T.; Haaland, A.; Schilling, B. E. R. *J. Chem. Soc., Dalton Trans.* **1986**, 2387.

(9) Fjeldberg, T.; Hope, H.; Lappert, M. F.; Power, P. P.; Thorne, A. J. *J. Chem. Soc., Chem. Commun.* **1983**, 639. (b) Chorley, R. W.; Hitchcock, P. B.; Lappert, M. F.; Leung, W.-P.; Power, P. P.; Olmstead, M. M. *Inorg. Chim. Acta* **1992**, *201*, 121.

(10) Kemp, R. A. Ph.D. Dissertation, The University of Texas at Austin, 1982. *Diss. Abstr., Int. B* **1982**, *43*(3), 718.

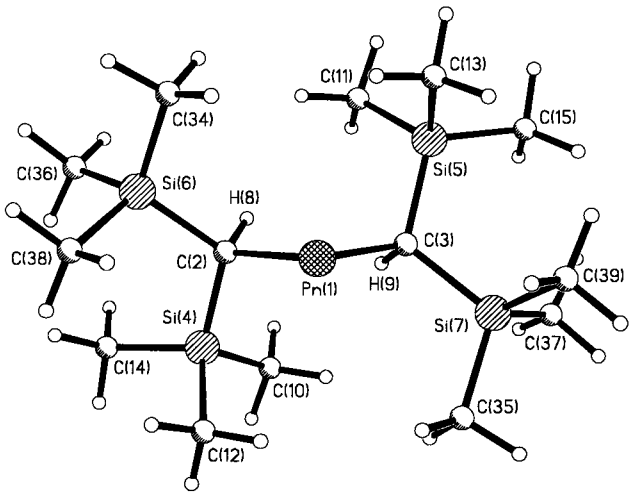

Figure 1. Gas-phase electron diffraction structures of **2** (Pn = P) and **4** (Pn = As); R = $CH(SiMe_3)_2$.

defined in an identical fashion. The electron diffraction refinements for both radicals were carried out by employing the minimum energy C_2 geometry for **2**, computed by ab initio methods, as the starting basis. The large number of geometric parameters needed to define the models made it necessary to assume that all the methyl groups are equivalent and possess local C_{3v} symmetry. Initially, some of the differences between related bond lengths and bond angles were restrained using the SARACEN[11] method. However, many of these parameters proved to be uncorrelated with other parameters and resulted in values and estimated standard deviations (ESD's) that were close to the restraints. In such cases, the values were fixed in the final refinement. The atom numbering protocol for radicals **2** and **4** is displayed in Figure 1 and selections of metrical parameters for both radicals are listed in Table 2. The r_α structures are not refined because the rectilinear vibrational corrections (i.e. parallel and perpendicular correction terms) are known to be unreliable for systems of these sizes that feature many low-frequency vibrational modes. Theoretical (UHF/3-21G*) Cartesian force fields were obtained for the local minima and converted into force fields described by a set of symmetry coordinates, using a version of the ASYM40[12] program that was modified for molecules with more than 40 atoms. In total, 27 geometric parameters and 46 groups of vibrational amplitudes were refined for **2**, and 27 geometric parameters and 27 groups of vibrational amplitudes were refined for **4**. Flexible restraints were employed during the refinements using the SARACEN[11] method. Overall, 25 geometric and 43 amplitude restraints were employed for **2** and 22 geometric and 24 amplitude restraints were employed for **4**; these are listed in the Supporting Information.

The success of the final refinements, for which $R_G = 6.9$ ($R_D = 5.7$) and 6.8 (5.4) for **2** and **4**, respectively, can be assessed on the basis of the radial distribution curves shown in Figure 2, and by reference to the molecular scattering intensity curves in the Supporting Information. The final refined parameters, interatomic distances and the corresponding amplitudes of vibration, and the least-squares correlation matrices are also presented in the Supporting Information.

Theoretical Calculations. All calculations at the UHF/3-21G*,[13−15] UHF/6-31G*,[16−18] UHF/DZP, and UB3LYP/DZP levels of theory were accomplished using the Gaussian 94 program.[19] The calculations were performed either on a Dec Alpha 1000 4/200 workstation or by use of the resources of the U.K. Computational Chemistry Facility, on a DEC 8400 superscalar cluster equipped with 10 fast processors, 6 GB of memory, and a 150 GB disk.

Graded series of geometry optimizations were undertaken for both the phosphinyl (**2**) and the arsinyl (**4**) radicals, from which the effect of increasing the quality of the basis set and the level of theory could be assessed. Geometry optimizations were undertaken initially at the UHF level using the standard 3-21G* and 6-31G* basis sets. Unless indicated otherwise, the geometries and energies reported herein were calculated at the UB3LYP/DZP level with a basis set designated "DZP", which comprises a 6-311G* [20,21] basis set for the phosphorus or arsenic atoms and a 6-31G* basis set for the carbon, silicon, and hydrogen atoms.

Vibrational frequencies were calculated from analytic second derivatives at the UHF/3-21G* level to determine the nature of stationary points for the models of **2** and **4** and to provide estimates of the amplitudes of vibration (u) for use in the GED refinements (see above). The C_2 symmetry structures were confirmed as the local minima for both radicals.

Table 2. Selected Bond Lengths (Å) and Bond Angles (deg) for the Radicals $^{\bullet}PR_2$ (**2**) and $^{\bullet}AsR_2$ (**4**) As Determined by Gas-Phase Electron Diffraction; R = $CH(SiMe_3)_2$

	2	**4**
Pn(1)-C(2)	1.856(11)	1.986(8)
C(2)−Si(4)	1.905(2)	1.893(2)
C(2)−Si(6)	1.902(2)	1.891(2)
Si(4)−C(10)	1.878(2)	1.871(2)
Si(4)−C(12)	1.878(2)	1.873(2)
Si(4)−C(14)	1.876(2)	1.873(2)
Si(6)−C(34)	1.880(2)	1.869(2)
Si(6)−C(36)	1.879(2)	1.873(2)
Si(6)−C(38)	1.875(2)	1.875(2)
C(2)−Pn(1)−C(3)	104.0(10)	101.2(10)
Pn(1)−C(2)−Si(4)	109.1(4)	111.8(6)
Pn(1)−C(2)−Si(6)	109.8(4)	112.1(6)
Pn(1)−C(2)−H(8)	108.1(13)	106.4(12)
Si(4)−C(2)−Si(6)	117.5(3)	117.3(3)
Si(4)−C(2)−H(8)	106.0(6)	104.1(6)
Si(6)−C(2)−H(8)	106.0(6)	104.0(6)
C(2)−Si(4)−C(10)	109.9(3)	111.7(3)
C(2)−Si(4)−C(12)	112.1(3)	110.5(3)
C(2)−Si(4)−C(14)	112.7(3)	111.8(3)
C(10)−Si(4)−C(12)	106.4(3)	108.7(3)
C(10)−Si(4)−C(14)	108.5(3)	107.2(3)
C(12)−Si(4)−C(14)	106.8(3)	106.9(3)
C(2)−Si(6)−C(34)	110.3(3)	113.3(3)
C(2)−Si(6)−C(36)	112.3(3)	110.4(3)
C(2)−Si(6)−C(38)	112.8(3)	110.7(3)
C(34)−Si(6)−C(36)	105.1(3)	108.2(3)
C(34)−Si(6)−C(38)	107.8(3)	106.4(3)
C(36)−Si(6)−C(38)	108.2(3)	107.7(3)
C(3)−Pn(1)−C(2)−H(8)	−26.4(8)	−25.3(9)

Results and Discussion

Gas-Phase Electron Diffraction (GED) Structures of $^{\bullet}PR_2$ and $^{\bullet}AsR_2$ Radicals (R = $CH(SiMe_3)_2$). Both radicals adopt a

(11) (a) Blake, A. J.; Brain, P. T.; McNab, H.; Miller, J.; Morrison, C. A.; Parsons, S.; Rankin, D. W. H.; Robertson, H. E.; Smart, B. A. *J. Phys. Chem.* **1996**, *100*, 12280. (b) Brain, P. T.; Morrison, C. A.; Parsons, S.; Rankin, D. W. H. *J. Chem. Soc., Dalton Trans.* **1996**, 4589.

(12) Hedberg, L.; Mills, I. M. *J. Mol. Spectrosc.* **1993**, *160*, 117.

(13) Binkley, J. S.; Pople, J. A.; Hehre, W. J. *J. Am. Chem. Soc.* **1980**, *102*, 939.

(14) Gordon, M. S.; Binkley, J. S.; Pople, J. A.; Pietro, W. J.; Hehre, W. J. *J. Am. Chem. Soc.* **1982**, *104*, 2797.

(15) Pietro, W. J.; Francl, M. M.; Hehre, W. J.; Defrees, D. J.; Pople, J. A.; Binkley, J. S. *J. Am. Chem. Soc.* **1982**, *104*, 5039.

(16) Hehre, W. J.; Ditchfield, R.; Pople, J. A. *J. Chem. Phys.* **1972**, *56*, 2257.

(17) Hariharan, P. C.; Pople, J. A. *Theor. Chim. Acta* **1973**, *28*, 213.

(18) Gordon, M. S. *Chem. Phys. Lett.* **1980**, *76*, 163.

(19) Frisch, M. J.; Trucks, G, W.; Schlegel, H. B.; Gill, P. M. W.; Johnson, B. G.; Robb, M. A.; Cheeseman, J. R.; Keith, T. A.; Petersson, G. A.; Montgomery, J. A.; Raghavachari, K.; Al-Laham, M. A.; Zakrzewski, V. G.; Ortiz, J. V.; Foresman, J. B.; Cioslowski, J.; Stefanov, B. B.; Nanayakkara, A.; Challacombe, M.; Peng, C. Y.; Ayala, P. Y.; Chen, W.; Wong, M. W.; Andres, J. L.; Replogle, E. S.; Gomperts, R.; Martin, R. L.; Fox, D. J.; Binkley, J. S.; Defrees, D. J.; Baker, J.; Stewart, J. P.; Head-Gordon, M.; Gonzalez, C.; Pople, J. A. *Gaussian 94*, Revision C.2; Gaussian Inc.: Pittsburgh, PA, 1995.

(20) McLean, A. D.; Chandler, G. S. *J. Chem. Phys.* **1980**, *72*, 5639.

(21) Krishnan, R.; Binkley, J. S.; Seeger, R.; Pople, J. A. *J. Chem. Phys.* **1980**, *72*, 650.

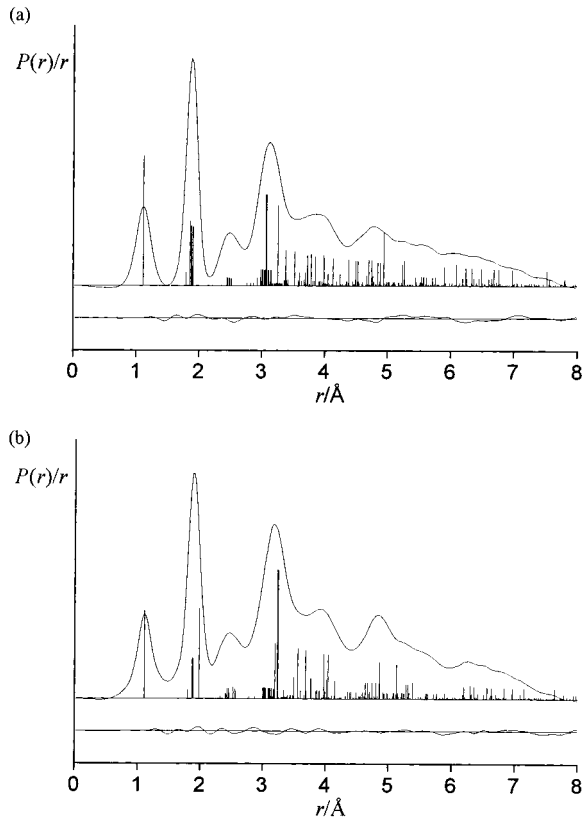

Figure 2. Experimental and difference (experimental − theoretical) radial-distribution curves, $P(r)/r$, for (a) $^{\bullet}PR_2$ **(2)** and (b) $^{\bullet}AsR_2$ **(4)** [R = $CH(SiMe_3)_2$]. Prior to Fourier inversion the data were multiplied by $s.\exp(-0.002s^2)/(Z_P - f_P)/(Z_{Si} - f_{Si})$ for $^{\bullet}PR_2$ and by $s.\exp(-0.002s^2)/(Z_{As} - f_{As})/(Z_{Si} - f_{Si})$ for $^{\bullet}AsR_2$.

V-shaped geometry. As expected on the basis of periodic group trends, the C−Pn−C bond angle of the phosphinyl radical **2** [104.0(10)°] is larger than that of the arsenic analogue **4** [101.2(10)°]. These angles are comparable to those that have been reported for X-ray crystallographic studies of the corresponding pnictide anions $[Li(\mu\text{-}PR_2)]_2$ [av. 102.0(5)°][22] and $[Li(\mu\text{-}AsR_2)]_3$ [98.1(8) and 100.8(9)°],[23] which are related to **2** and **4** by one-electron reduction. Within experimental error, the P−C and As−C bond lengths of 1.856(11) and 1.981(8) Å for **2** and **4**, respectively, are indistinguishable from those determined by GED for less sterically encumbered neutral compounds such as PMe_3 [1.847(3) Å][24] and $AsMe_3$ [1.968(3) Å][25] despite the fact that the coordination number of **2** and **4** is only two, in contrast to the three-coordinate pnictogen atom in PMe_3 or $AsMe_3$. The conformations of the radicals are of particular importance in terms of assessing the changes that accompany dimerization. The orientations of the $CH(SiMe_3)_2$ ligands around the Pn−C bonds are best described in terms of the dihedral angles C(3)−P(1)−C(2)−H(8) and C(3)−As(1)−C(2)−H(8) which are 26.4(8)° and 25.3(9)° for **2** and **4**, respectively. Thus both radicals possess *syn*,*syn* conformations in which the pair of methine hydrogen atoms point toward the middle of the V-shaped C−Pn−C skeleton. Such a conformation minimizes strong interligand interactions as evidenced by the observation that the average C−Si−C bond angles for both **2** [111.7(3)°] and **4** [111.2(3)°] are close to the ideal tetrahedral value. Moreover, the average $Si-C_{methyl}$ bond lengths for **2** [1.878(2) Å] and **4** [1.872(2) Å] are comparable to those determined by GED for less sterically crowded molecules such as 1,4-disilabutane [1.882(1) Å][26] and 1,5-disilapentane [1.886(1) Å].[26] However, the observation that the average $Si-C_{methine}$ bond lengths for **2** [1.904(2) Å] and **4** [1.892(2) Å] exceed those for the $Si-C_{methyl}$ bonds [1.877(2) Å for **2**; 1.872(2) Å for **4**], which finds a parallel in the structures of GeR_2 and SnR_2 [R = $CH(SiMe_3)_2$],[8a] may be due to intraligand strain relief. Taken collectively, however, there is very little evidence of residual strain associated with either of the pnictinyl radical structures.

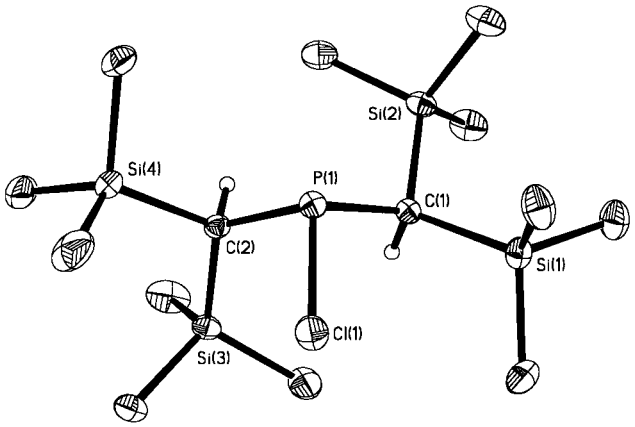

Figure 3. Molecular structure of R_2PCl **(5)** showing the atom numbering scheme [R = $CH(SiMe_3)_2$]. The structure of R_2AsCl (**6**) is isotypical.

Solid State Structural Investigations. Single-crystal X-ray diffraction experiments were performed on the dipnictines **1** and **3** to assess the structural changes that occur upon dimerization of the corresponding radicals **2** and **4**, bearing in mind, of course, that the dimerization also involves a change from the gas to the solid state. It was also considered useful to determine the X-ray crystal structures of the chloropnictine starting materials (**5**, Pn = P; **6**, Pn = As) to provide comparative metrical parameters for R_2Pn fragments attached to significantly smaller substituents (Cl vs R_2Pn).

Chloropnictines 5 and 6. The molecular structures of **5** and **6** are isotypical and each chloropnictine possesses the expected pyramidal geometry (Figure 3 and Table 4), as reflected by the sums of angles at the group 15 center (308.8° for **5** and 303.6° for **6**). In each molecule, one $CH(SiMe_3)_2$ ligand [(based on C(1))] is oriented in a fashion very similar to that adopted by both such ligands in radicals **2** and **4**. However, the second $CH(SiMe_3)_2$ ligand [(based on C(2))] is twisted around the Pn−C bond by approximately 30° in order to reduce the contact with the chlorine atom. Overall, each chloropnictine possesses a roughly *syn*,*syn* orientation of $CH(SiMe_3)_2$ ligands in the solid state, similar to that of the corresponding pnictinyl radicals in the gas phase. This observation suggests that in the absence of significant steric loading at the Pn atom, the preferred orientation of the PnR_2 fragment is similar regardless of the phase—presuming, of course, that a similar situation exists in solution. No significant intermolecular interactions are observed in either structure and the geometrical parameters for each compound are unexceptional. Interestingly, **5** and **6** represent rare examples

(22) Hitchcock, P. B.; Lappert, M. F.; Power, P. P.; Smith, S. J. *J. Chem. Soc., Chem. Commun.* **1984**, 1669.

(23) Hitchcock, P. B.; Lappert, M. F.; Smith, S. J. *J. Organomet. Chem.* **1987**, *320*, C27.

(24) McAdam, A.; Beagley, B.; Hewitt, T. G. *Trans. Faraday Soc.* **1970**, *66*, 2732.

(25) Downs, A. J.; Hunt, N. I.; McGrady, G. S.; Rankin, D. W. H.; Robertson, H. E. *J. Mol. Struct.* **1991**, *248*, 393.

(26) See, for example: Mitzel, N. W.; Smart, B. A.; Blake, A. J.; Robertson, H. E.; Rankin, D. W. H. *J. Phys. Chem.* **1996**, *100*, 9339.

Table 3. Selected Metrical Parameters (angles in deg and bond lengths in Å) with Mean Values and Root-Mean-Square Deviations for Molecules #1 and #3−#8 of **3** Compared with the Values for Molecule #2 of **3** and **1**; R = $[CH(SiMe_3)_2]$

parameter	min.	max.	mean	typical ESD	RMS deviation	#2 As_2R_4	P_2R_4
Pn(n1)−Pn(n2)	2.5755	2.5922	2.5867	0.0016	0.005	2.5384(16)	2.3103(7)
Pn(n1)−C(n1)	2.011	2.060	2.038	0.006	0.019	2.027(10)	1.892(2)
Pn(n1)−C(n2)	2.023	2.056	2.043	0.009	0.009	2.024(6)	1.896(2)
Pn(n2)−C(n4)	2.011	2.042	2.024	0.008	0.009	2.030(11)	1.892(2)
Pn(n2)−C(n3)	2.020	2.060	2.034	0.008	0.012	2.035(7)	1.893(2)
C(n1)−Si(n1)	1.864	1.898	1.887	0.006	0.012	1.889(9)	1.905(2)
C(n1)−Si(n2)	1.894	1.921	1.907	0.005	0.008	1.888(8)	1.896(2)
C(n2)−Si(n3)	1.880	1.915	1.900	0.006	0.012	1.913(7)	1.915(2)
C(n2)−Si(n4)	1.874	1.914	1.897	0.009	0.015	1.865(8)	1.894(2)
C(n3)−Si(n5)	1.880	1.916	1.894	0.008	0.011	1.904(10)	1.926(2)
C(n3)−Si(n6)	1.863	1.917	1.889	0.008	0.015	1.897(8)	1.892(2)
C(n4)−Si(n8)	1.876	1.907	1.891	0.008	0.010	1.883(6)	1.896(2)
C(n4)−Si(n7)	1.888	1.914	1.904	0.008	0.011	1.925(7)	1.921(2)
C(n1)−Pn(n1)−C(n2)	101.6	102.4	102.1	0.3	0.5	102.6(3)	103.57(9)
C(n3)−Pn(n2)−C(n4)	103.4	104.5	103.9	0.3	0.4	103.6(3)	103.00(9)
Pn(n2)−P (n1)−C(n1)	102.5	104.2	103.4	0.2	0.6	104.3(2)	107.92(7)
Pn (n2)−Pn(n1)−C(n2)	104.6	106.0	105.4	0.2	0.5	103.2(2)	104.83(6)
Pn (n1)−Pn(n2)−C(n4)	102.8	104.3	103.5	0.2	0.6	103.5(2)	106.98(6)
Pn (n1)−Pn(n2)−C(n3)	102.4	105.5	103.3	0.2	1.0	103.6(3)	105.27(7)
Pn(n1)−C(n1)−Si(n1)	120.3	121.3	120.8	0.4	0.3	121.8(3)	123.33(11)
Pn(n1)−C(n1)−Si(n2)	113.6	114.0	113.8	0.3	0.3	109.7(4)	111.88(10)
Pn(n1)−C(n2)−Si(n3)	104.5	105.9	105.2	0.4	0.5	110.2(3)	112.35(10)
Pn(n1)−C(n2)−Si(n4)	129.7	132.0	130.6	0.3	0.7	125.0(4)	125.19(11)
Pn(n2)−C(n3)−Si(n5)	105.7	107.2	106.4	0.4	0.6	110.0(3)	112.83(11)
Pn(n2)−C(n3)−Si(n6)	116.2	119.2	117.7	0.3	1.1	123.4(6)	125.07(11)
Pn(n2)−C(n4)−Si(n7)	112.2	114.4	113.9	0.3	0.8	108.9(3)	110.88(10)
Pn(n2)−C(n4)−Si(n8)	120.6	121.5	121.0	0.4	0.4	123.2(4)	123.83(11)
C(n1)−Pn(n1)−C(n2)−H(n21)	−3.7	−7.5	−5.9	0.9	1.3	149.1(6)	156.3(17)
C(n2)−Pn(n1)−C(n1)−H(n11)	128.0	134.3	131.7	0.9	2.2	2.2(7)	7.8(16)
C(n3)−Pn(n2)−C(n4)−H(n41)	129.7	132.4	131.5	0.9	1.0	148.1(6)	149.4(16)
C(n4)−Pn(n2)−C(n3)−H(n31)	−15.0	−20.2	−17.3	0.9	1.9	3.7(8)	−4.6(17)
C(n1)−Pn(n1)−Pn(n2)−C(n3)	−137.9	−130.8	−133.8	0.3	2.1	−140.0(3)	−141.11(11)
C(n1)−Pn(n1)−Pn(n2)−C(n4)	−23.6	−30.8	−26.3	0.3	2.4	−32.0(3)	−32.0(1)
C(n2)−Pn(n1)−Pn(n2)−C(n3)	115.9	120.8	118.8	0.3	1.6	113.0(3)	108.98(11)
C(n2)−Pn(n1)−Pn(n2)−C(n4)	−132.6	−137.0	−133.9	0.3	1.7	−139.0(4)	−141.91(10)
Si(n1)−C(n1)−Pn(n1)−Pn(n2)	−87.1	−83.5	−85.1	0.5	1.1	−70.6(4)	−70.16(13)
Si(n2)−C(n1)−Pn(n1)−Pn(n2)	128.8	130.6	129.5	0.4	0.8	149.0(3)	149.76(8)
Si(n3)−C(n2)−Pn(n1)−Pn(n2)	−154.7	−150.7	−153.0	0.4	1.3	−141.8(4)	−138.30(9)
Si(n4)−C(n2)−Pn(n1)−Pn(n2)	−16.8	−10.8	−13.9	0.5	1.7	−3.6(6)	−1.93(14)
C(n11)−Si(n1)−C(n1)−Pn(n1)	46.3	50.3	48.4	0.6	1.3	−65.9(6)	−60.88(17)
C(n21)−Si(n2)−C(n1)−Pn(n1)	112.1	116.6	114.5	0.5	1.5	92.8(5)	93.32(15)
C(n31)−Si(n3)−C(n2)−Pn(n1)	−52.3	−46.7	−50.1	0.6	1.9	−10.6(8)	−5.83(16)
C(n41)−Si(n4)−C(n2)−Pn(n1)	137	142	139.7	0.5	1.6	175.7(5)	173.35(15)
Si(n8)−C(n4)−Pn(n2)−Pn(n1)	−88.6	−82.8	−85.4	0.5	2.0	−75.0(6)	−69.69(13)
Si(n7)−C(n4)−Pn(n2)−Pn(n1)	127.9	131.5	129.3	0.4	1.2	148.3(4)	151.06(8)
Si(n5)−C(n3)−Pn(n2)−Pn(n1)	−158	−153.4	−156.4	0.3	1.4	−139.4(3)	−140.98(11)
Si(n6)−C(n3)−Pn(n2)−Pn(n1)	−30.9	−25.8	−28.6	0.5	1.7	−3.4(4)	−2.12(18)
C(n81)−Si(n8)−C(n4)−Pn(n2)	45.3	51.3	48.5	0.7	2.0	64.8(7)	61.11(18)
C(n71)−Si(n7)−C(n4)−Pn(n2)	111.7	114.8	113.0	0.5	1.0	94.0(4)	93.93(13)
C(n51)−Si(n5)−C(n3)−Pn(n2)	−43.7	−38.3	−40.6	0.5	1.7	−15.9(4)	−9.63(19)
C(n61)−Si(n6)−C(n3)−Pn(n2)	80	85	82.2	0.7	1.8	−57.5(6)	−65.5(2)

of uncomplexed dialkylchloropnictines that have been characterized by X-ray crystallography, as confirmed by a search of the Cambridge Structural Database.[27]

Diphosphine 1. The molecular structure of **1** (Figure 4) reveals a number of exceptional features. For example, the P−P bond length [2.310(7) Å] is the longest yet reported for a diphosphine, being ∼ 0.1 Å longer than those reported for other uncoordinated diphosphines. In this context, exemplary comparative P−P bond lengths for $(PR'R'')_2$ include 2.260(1) Å (R′, R″ = Mes),[28] 2.215(3) Å (R′, R″ = Cy),[29] 2.211(2) and 2.206(2) Å (R′ = Ph, R″ = C(O)-*t*-Bu),[30] 2.212(1) Å (R′, R″ = Me),[31] 2.2051(11) Å (R′ + R″ = cyclo-$(CPh)_4$),[32] 2.246(2) Å (R′, R″ = CF_3),[33] and 2.2461(16) Å (R′, R″ = 2,4,6-*i*-PrC_6H_2).[34] However, our calculations suggest that a P−P lengthening of ∼0.1 Å corresponds to only ca. 4 kJ mol^{-1} destabilization of the P−P bond (see Supporting Information). Clearly, the observed facile dissociation into phosphinyl radicals must reflect the release of steric strain in other parts of the diphosphine.

(27) Allen, F. H.; Kennard, O. *Chem. Design Automation News* **1993**, *8*, 131.
(28) Baxter, S. G.; Cowley, A. H.; Davis, R. E.; Riley, P. E. *J. Am. Chem. Soc.* **1981**, *103*, 1699.
(29) Richter, R.; Kaiser, J.; Sieler, J.; Hartung, H.; Peter, C. *Acta Crystallogr.* **1977**, *B33*, 1887.
(30) Becker, G.; Mundt, O.; Rössler, M. *Z. Anorg. Allg. Chem.* **1980**, *468*, 55.
(31) Mundt, O.; Riffel, H.; Becker, G.; Simon, A. *Z. Naturforsch.* **1988**, *43b*, 952.
(32) Vohs, J. K.; Wei, P.; Su, J.; Beck, B. C.; Goodwin, S. D.; Robinson, G. H. *Chem. Commun.* **2000**, 1037.
(33) Becker, G.; Golla, W.; Grobe, J.; Klinkhammer, K. W.; Le Van, D.; Maulitz, A. H.; Mundt, O.; Oberhammer, H.; Sachs, M. *Inorg. Chem.* **1999**, *38*, 1099.
(34) Brady, F. J.; Cardin, C. J.; Cardin, D. J.; Wilcock, D. J. *Inorg. Chim. Acta* **2000**, *298*, 1.

Table 4. Selected Bond Lengths (Å) and Bond Angles (deg) for the Chloropnictines R_2PCl (**5**) and R_2AsCl (**6**); R = $CH(SiMe_3)_2$

	5	**6**
Pn(1)−Cl(1)	2.1192(6)	2.2309(10)
Pn(1)−C(1)	1.8369(18)	1.980(3)
Pn(1)−C(2)	1.8473(17)	1.980(3)
C(1)−Si(1)	1.9087(18)	1.897(3)
C(1)−Si(2)	1.9165(18)	1.908(3)
C(2)−Si(3)	1.9038(18)	1.891(3)
C(2)−Si(4)	1.9074(19)	1.903(3)
C(1)−Pn(1)−C(2)	106.00(8)	103.10(13)
C(1)−Pn(1)−Cl(1)	105.28(6)	103.16(10)
C(2)−Pn(1)−Cl(1)	97.73(6)	97.32(10)
Pn(1)−C(1)−Si(1)	113.75(9)	113.31(16)
Pn(1)−C(1)−Si(2)	108.33(9)	107.38(16)
Si(1)−C(1)−Si(2)	112.92(9)	113.94(15)
Pn(1)−C(2)−Si(3)	121.94(10)	121.95(17)
Pn(1)−C(2)−Si(4)	107.89(9)	106.32(16)
Si(3)−C(2)−Si(4)	115.27(9)	115.24(16)
C(2)−Pn(1)−C(1)−H(1)	29.1(14)	26.3
C(1)−Pn(1)−C(2)−H(2)	52.6(13)	51.5

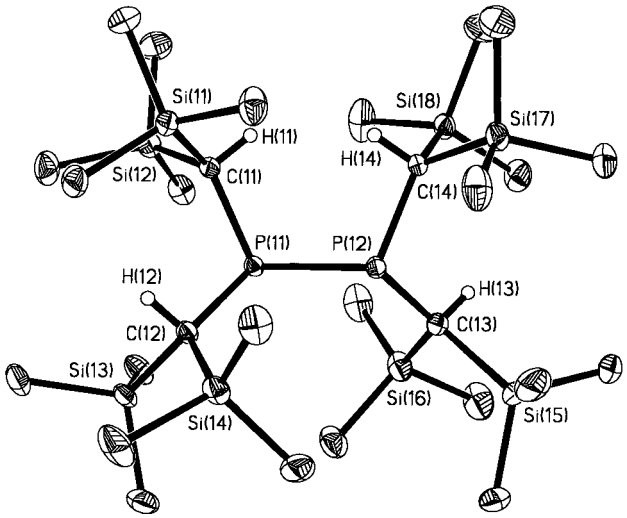

Figure 4. Molecular structure of $(PR_2)_2$ **(1)** showing the atom numbering scheme [R = $CH(SiMe_3)_2$]. Most of the hydrogen atoms are omitted for clarity.

Undoubtedly, the most interesting feature of the molecular structure of diphosphine **1** is the *syn,anti* orientation [C(14)−P(12)−C(13)−H(13) = −4.6(2)°, C(13)−P(12)−C(14)−H(14) = 149.4(2)°] of the $CH(SiMe_3)_2$ ligands on each PR_2 fragment. Such an arrangement allows for more efficient packing of the ligands in the dimer than does the *syn,syn* conformation, which is found in the case of the monomeric radical **2** [C(3)−P(1)−C(2)−H(8) = 26°]. However, the consequence of this packing is that substantial steric strain exists (a) within each $CH(SiMe_3)_2$ ligand, i.e. between the two trimethylsilyl groups, (b) between the two $CH(SiMe_3)_2$ ligands attached to each phosphorus atom, and (c) between the $CH(SiMe_3)_2$ ligands on the two halves of the molecule. That the strain is much greater in the diphosphine than in the radical can be appreciated by considering the angular distortions at the silicon atoms and the methine carbon atoms in the two species. A comprehensive listing of individual angles appears in the Supporting Information; however, the effects are illustrated by the root-mean-square (RMS) variances from the means of the angles at the methine carbon and silicon atoms. In radical **2**, these values are 3.88° and 2.55°, respectively, whereas in the corresponding diphosphine **1** they are 17.96° and 4.06°. There are also increases in many of the bond lengths in the $CH(SiMe_3)_2$ ligands of the diphosphine, with the largest increases being closer to the molecular core. For example, the P−C distance is almost 0.04 Å longer in **1** [1.892 (2) and 1.896 (2) Å] than in **2** [1.856(11) Å]. In this light, the significantly deformed $CH(SiMe_3)_2$ ligands can be considered to represent a store of potential energy, most of which can be released to effect the dissociation of dimer upon melting, vaporization, or dissolution in a solvent. The theoretical aspects of this effect are explored in a subsequent section. It is important to note that the diphosphines with other types of sterically demanding ligands, such as $(PCy_2)_2$,[29] $(PMes_2)_2$,[28] $(P\text{-}t\text{-}Bu_2)_2$,[31] and $(P(CPh)_4)_2$,[32] maintain P−P bonding in solution. Moreover, $(PMe_2)_2$ and $[P(CF_3)_2]_2$ remain intact in the vapor phase.[33,36]

The conformation of **1** and the remaining metrical parameters are comparable to those reported for other bulky diphosphines. For example, the partially eclipsed anti arrangement (as viewed down the P−P bond) of the $CH(SiMe_3)_2$ ligands in **1** is similar to the geometries observed for $(PMes_2)_2$,[28] $(PCy_2)_2$,[29] and $[P\{C(O)\text{-}t\text{-}Bu\}Ph]_2$.[30] The extent of eclipsing in the case of **1**, as revealed by the C(11)−P(11)−P(12)−C(14) dihedral angle of 32.0(1)°, falls between those of $(PCy_2)_2$ (5.5°)[29] and $(PMes_2)_2$ (50.8°).[28] As expected, the C(12)−P(11)−P(12)−C(13) dihedral angle of 109.0(1)° for **1** also lies between the values of the corresponding angles reported for $(PCy_2)_2$ (137.6°)[29] and $(PMes_2)_2$ (94.4°).[28] Diphosphines with appreciably less bulky ligands, such as Me or CF_3, possess more symmetrical (trans, C_{2h}) geometries, thus suggesting that the twisting from the ideal arrangement is controlled by the packing requirements of the ligands. The C−P−C angles in **1** [103.6(9)° and 103.0(9)°] are indistinguishable from those in $(PCy_2)_2$ [103.1(3)° and 103.8(4)°][29] and $(PMes_2)_2$ [103.5(2)°].[28]

Diarsine 3. The solid state of **3** features the presence of eight independent molecules in the asymmetric unit. However, each molecule adopts a *syn,anti* conformation as in the case of diphosphine **1**. Specifically, each arsinyl moiety has one $CH(SiMe_3)_2$ ligand twisted by ∼15° in one direction while the other is twisted by ∼130° in the opposite direction with respect to eclipsing of the C−H and P−P bonds (0°). The significance of this observation is that it demonstrates that the *syn,anti* arrangement is still necessary despite the larger size of arsenic, thus supporting our preliminary conclusions regarding the role of the $CH(SiMe_3)_2$ ligands in the phosphinyl radical/diphosphine system (see Introduction).

The presence of a relatively large number of crystallographically independent molecules that were structurally characterized under identical experimental conditions afforded a rare opportunity to assess the effects of crystal packing by scrutiny of the variations in dihedral angles, bond angles, and bond lengths among the eight individual molecules. All eight molecules were found to possess approximately C_2 symmetry, and in fact, molecule #2 possesses this symmetry almost exactly. The remaining molecules, which are essentially identical to each other, deviate from C_2 symmetry primarily in terms of the torsion angles about the C(n2)−Si(n4) and related C(n3)−Si(n6) bonds. (See Figure 5 for the atom numbering scheme.) The structures of molecule #1 (∼C_2 symmetry) and molecule #2 (C_2 symmetry) are compared in Figure 6.

Since molecule #2 was found to be significantly different from the other seven it was omitted from the statistical analysis. The average values for most of the dihedral angles, bond angles,

(35) (a) Aime, S.; Harris, R. K.; McVicker, E. M.; Fild, M. *J. Chem. Soc., Chem. Commun.* **1974**, 426. (b) Brunelle, J. A.; Bushweller, C. H.; English, A. D. *J. Phys. Chem.* **1976**, *80*, 2598.

(36) Cowley, A. H.; Dewar, M. J. S.; Goodman, D. W.; Padolina, M. C. *J. Am. Chem. Soc.* **1974**, *96*, 2648.

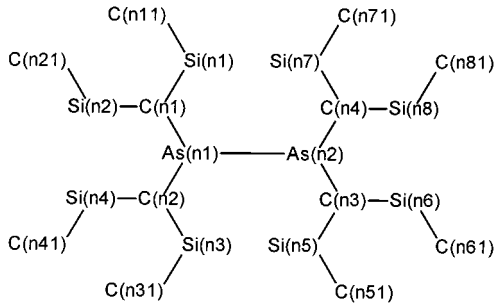

Figure 5. Numbering system for the eight independent molecules of $(AsR_2)_2$, where $n = 1-8$.

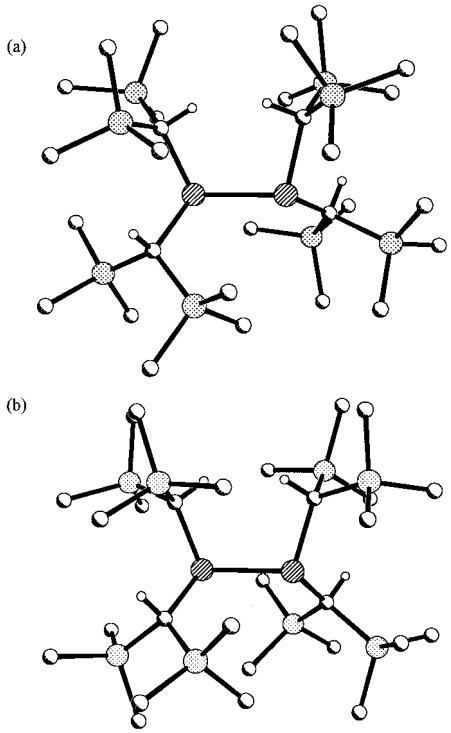

Figure 6. Molecular structures of molecules #1 and #2 of $(AsR_2)_2$ [R = $CH(SiMe_3)_2$].

and bond lengths were determined for the other seven molecules. A summary of the analyses of these metrical parameters, along with pertinent RMS deviations, is presented in Table 3. Note that the RMS deviations for the sets of dihedral angles average 1.5° and that the deviations for the individual parameters are consistently close to their respective mean values. The RMS deviations compare to the mean ESD of 0.5° for the crystallographically determined dihedral angles. Clearly there is remarkably little variation in dihedral angles among the seven molecules and only ~1.0° of the variation in each dihedral angle can be attributed to packing effects. The foregoing analysis leads to the conclusion that there is no significant torsional freedom within the molecules. In fact, none of the eight trimethylsilyl groups in any given molecule can rotate freely, a situation that is unusual and highlights the control of ligand close-packing on the solid-state structure.

The mean of RMS differences for the sets of angles is 0.7°, compared with the mean ESD of 0.5° for the measured angles. On average, therefore, only ~ 0.2° of the distortion of any one angle can be attributed to packing effects. Thus, the observed differences between angles at any given atom are due to molecular structure effects and not to crystal packing. Examination of the mean As−C−Si angles in related moieties illustrates this point well. For example, the mean As(n1)−C(n1)−Si(n1) angle is 120.8° whereas the As(n1)−C(n1)−Si(n2) angle averages 113.8°. These values agree well with the related halves of the molecules [As(n2)−C(n4)−Si(n8/n7) = 121.0 and 113.9°, respectively]. Furthermore, these angles are all in the upper, less-crowded, half of the molecule that contains both *anti* $CH(SiMe_3)_2$ ligands as illustrated in Figure 6. However, in the lower halves of the molecules, which contain both *syn* $CH(SiMe_3)_2$ ligands, the angles As(n1)−C(n2)−Si(n3/n4) were observed to average 105.2(5) and 130.7(7)°, respectively, compared with As(n2)−C(n3)−Si(n5/n6) [106.4(6) and 117.7(11)°, respectively]. Not only is the difference between the two As−C−Si angles around each C(n2) atom enlarged considerably (by 24−27° difference in each of the seven molecules), but it is also clear that it is the ~130° angle to Si(n4) that is the most distorted.

Regarding the $C_{methine}-Si-C_{methyl}$ angles, the greatest distortions are also observed around Si(n4), with angles ranging from 105.9 to 118.2° compared with a range of 109.2−113.5° for the related Si(n6) atom. Analysis of the $C_{methyl}-Si-C_{methyl}$ angles yields another surprising result, namely that the range of angles about Si(n6) is greater (103.9−111.0°) than that about Si(n4) (104.8−107.4°). In contrast, all the other ranges of angles for both (R_2As) moieties of the diarsine molecules were found to be mutually consistent. Furthermore, the seven molecules display an average RMS difference of 0.013 Å for the sets of bond lengths compared with the typical ESD of 0.008 Å. As in the case of **1**, all the $C_{methine}-Si$ bond lengths are longer than the $C_{methyl}-Si$ distances in the trimethylsilyl groups and there is no significant variation in the corresponding Si−C bond lengths between the seven independent diarsine molecules.

Overall, the conclusion that emerges from the statistical analysis of the seven independent molecules of **3** is that packing effects cause, on average, a change of roughly 0.005 Å in all bond lengths, 0.2° in all bond angles, and 1.0° in all torsion angles. Moreover, there are very large distortions that are common to all seven molecules (and largely related in the eighth molecule). These distortions, most markedly the angles at C(n2), Si(n4), and Si(n6), allow the trimethylsilyl groups to mesh together within the overall framework of the molecule. Such a restricted conformational freedom is an unusual feature and is a manifestation of the steric strain within this molecule. As in the case of diphosphine **1**, the As−As bond lengths for **2**, which average 2.587 Å [2.576(2) to 2.592(2) Å range], are ~ 0.1 Å longer than those reported for other diarsines (CSD average 2.455 Å; 2.417−2.489 Å range).[27]

As illustrated in Figure 6b, the $SiMe_3$ groups of molecule #2 of the diarsine adopt different conformations than those in the other seven molecules. In turn, this results in a significantly shorter As−As bond length [2.538(2) Å] and the adoption of almost exact C_2 symmetry. Furthermore, the metrical parameters and conformational preference of diarsine molecule #2 are remarkably similar to those of the analogous diphosphine **1**, as demonstrated in Table 3. It seems that the slightly longer As−As bond (with a presumably more shallow torsional potential energy surface) permits slight variations of the required *syn,-anti* conformation that are not observed in the case of the diphosphine.

Theoretical Aspects of the Dissociation Process, $R_4Pn_2 \rightarrow 2\ ^{\bullet}PnR_2$. To gain more quantitative insights into the energetics of the structural changes accompanying the dipnictine-to-pnictinyl radical dissociation process, it was important to probe an appropriate system using quantum chemical methods. Because of the similar behavior of the phosphorus and arsenic

Table 5. Summary of Theoretical Results at the UB3LYP/DZP Level of Theory

conformational description	label	energy/ au = hartree	relative energy/ kJ mol^{-1}	P−P cleavage energy/ kJ mol^{-1}
R_2P-PR_2, single point energy[b]	**1**	−4111.49606999	0.00 (1/2 of **1**)	95.87
syn,anti-•PR_2 radicals, single point energy[b]	**1A$_1$**	−2055.73639389	30.56	
	1A$_2$	−2055.72315900	65.31	
syn,anti-•PR_2 radical, H optimized, heavy atoms fixed[c]	**1B$_2$**	−2055.81424078	84.18	
syn,anti-•PR_2 radical, fully optimized[d]	**1C**	−2055.83386190	32.66	
syn,syn- •PR_2 radicals, fully optimized[d]	**2**	−2055.84630210	0.00	
Me_2P-PMe_2, fully optimized, C_2h symmetry	**7**	−842.4185108	0.00	208.03
PMe_2 radicals, single point energy[e]	**7A**	−421.1696384	104.01	
PMe_2 radicals, fully optimized, C_2v symmetry	**8**	−421.1701774	102.60	

[a] "R_2P-PR_2" refers to *syn,anti*-$(PR_2)_2$ and "radical" refers to •PR_2 where R = $CH(SiMe_3)_2$. [b] All atoms in the experimentally determined positions, except for hydrogens, for which C−H distances were fixed at 1.08 Å. [c] Heavy atoms fixed in the experimentally determined positions, H atoms allowed to optimize. [d] All atoms allowed to optimize. [e] Atomic positions from optimization of **7**.

analogues, the calculations were restricted to the systems $R_4P_2 \rightarrow 2\ ^{\bullet}PR_2$ [R = $CH(SiMe_3)_2$] and $Me_4P_2 \rightarrow 2\ ^{\bullet}PMe_2$.

A search of the potential energy surface of **2** led to the location of one minimum with C_2 symmetry. Vibrational frequency calculations at the UHF/3-21G* level confirmed that this structure represents a local minimum on the potential energy surface. The metrical parameters for **2** proved to be relatively insensitive to the theoretical method; selected metrical parameters obtained from the UB3LYP/DZP calculation are listed in the Supporting Information along with those calculated at the UHF/6-31G* and UHF/DZP levels of theory. In general, there is a very good agreement between the calculated and observed structures.[37] Typically, the calculated angles fall within 1−2° of the GED values and the computed bond lengths are approximately 0.01−0.02 Å longer than the experimental values, even though the calculated equilibrium distances must be slightly shorter than the vibrationally averaged r_a distances. For example, the P−C bond length refined to 1.856(11) Å, compared with the computed value of 1.876 Å, and the experimental range of C−Si bond lengths is 1.875−1.905 Å, compared with the calculated range of 1.894−1.926 Å. The C−P−C angle refined to 104.0(10)° vs the calculated angle of 104.8°. The experimental dihedral angle C(3)−P(1)−C(2)−H(8) of −26.4(8)° agrees very well with the calculated value of −26.6° and the conclusion that **2** adopts a *syn,syn* conformation in which both methine hydrogen atoms point toward the middle of the V-shaped C−P−C skeleton.

A full geometry optimization for diphosphine **1** was not feasible using the available resources. Accordingly, the theoretical modeling of **1** is restricted to single-point calculations at the crystallographically determined geometry (with heavy atoms fixed in the crystallographically determined geometry and C−H bond lengths fixed at 1.08 Å).

An energy diagram summarizing the results of the $R_4P_2 \rightarrow 2\ ^{\bullet}PR_2$ dissociation process is presented in Figure 7 and the calculated energies are listed in Table 5. Dissociation of the dimer into the two fragments via cleavage of the P−P bond, **1A$_1$** and **1A$_2$**, yields a P−P homolysis energy of 96 kJ mol^{-1}. The hydrogen atom positions in **1A$_2$** were then allowed to optimize to give **1B$_2$** (**1A$_2$** and **1B$_2$** are more distorted than **1A$_1$** and **1B$_1$** and thus provide larger energy differences). This energy change, which reflects the correction for the difference between the experimental (X-ray diffraction, with C−H distances corrected to 1.08 Å) and theoretical hydrogen atom positions in the PR_2 moiety, is 239 kJ mol^{-1}, and it was assumed to be the same for the other monomer (and presumably approximately twice this value for **1**).[38] The heavy atom and hydrogen atom positions for **1B$_2$** were then allowed to relax to give the optimized structure of the phosphinyl radical with the *syn,anti* conformation (**1C$_2$**). This optimization releases 52 kJ mol^{-1}, corresponding to an estimate of 17 kJ mol^{-1} for **1B$_1$** (Figure 7), since **1C$_1$** and **1C$_2$** must be identical by definition. Finally, rotation of one of the R ligands around the P−C bond to form the optimized *syn,syn* conformation (**2**), analogous to that observed experimentally, releases a further 33 kJ mol^{-1} per radical. Thus, while the initial step in the homolysis reaction is endothermic, the relaxation and rotation of the R ligands releases at least 135 kJ mol^{-1} (per dimer), which is more than sufficient to render the overall process exoergic. Furthermore, at temperatures >0 K, $T\Delta S$ will be positive due both to the increase in the number of species and fewer constraints on ligand motion in the radical compared with the dimer.

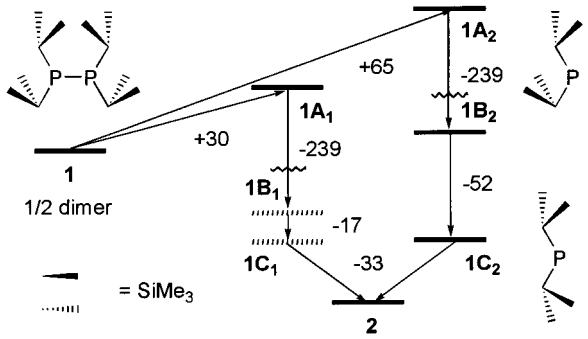

Figure 7. Schematic summary of DFT calculation results for diphosphine **1** in the solid-state geometry, the *syn,anti* phosphinyl radicals with solid-state geometries (**1A$_1$** and **1A$_2$**) and with hydrogen atom positions relaxed (**1B$_1$** and **1B$_2$**), the *syn,anti* phosphinyl radical in the optimized geometry (**1C**; the same for both radical fragments), and the *syn,syn* phosphinyl radical in the optimized geometry **2**. Energies are in kJ mol^{-1}.

An analogous series of calculations was performed on the nonbulky system $Me_4P_2 \rightarrow 2\ ^{\bullet}PMe_2$ for comparative purposes. As shown in Table 5, replacement of the bulky $CH(SiMe_3)_2$ ligands by methyl ligands increases the phosphine homolysis energy to 208 kJ mol^{-1}. As expected on the grounds of steric repulsions, this $Me_4P_2 \rightarrow 2\ ^{\bullet}PMe_2$ homolysis energy is larger than that computed for **1** → **2** (96 kJ mol^{-1}). However, it should be borne in mind that the latter value is probably underestimated because the larger system was calculated on the basis of nonoptimized structures. More importantly, in contrast to the **1**

(37) An analogous series of calculations was performed on the arsinyl radical **4**; the metrical parameters calculated at the UB3LYP/DZP level of theory are listed in the Supporting Information.

(38) Note that although the contribution from H-atom relaxation cannot yet be assessed explicitly, it is likely that the energy of relaxation in diphosphine **1** will roughly cancel out the energies of relaxation of the individual moieties and can safely be neglected.

→ **2** process, the $Me_4P_2 \rightarrow 2\ ^{\bullet}PMe_2$ calculations reveal that the energy of the entire dissociation process is highly *endothermic* (205 kJ mol^{-1}) and comparable to the homolysis energy. The magnitudes of both energies are nearly identical because of the almost insignificant (<1.5 kJ mol^{-1}) release of energy for the relaxation of the $^{\bullet}PMe_2$ fragment after dissociation.

Overall, these calculations show that simple P−P bond dissociation of the diphosphine is thermodynamically unfavorable. Furthermore, the steric strain potential energy, which is stored by virtue of the deformation of the flexible and asymmetric $CH(SiMe_3)_2$ ligands, is released in solution or the gas phase to effect dissociation of the dipnictine. In fact, this release of energy is sufficient to render the pair of radicals more *thermodynamically* stable than the diphosphine in less condensed media.

Conclusions

The size, shape, and facile deformation of the $CH(SiMe_3)_2$ ligands are the most important factors that determine the unusual properties of diphosphine **1** and diarsine **3**. In contrast to the conventional understanding of sterically demanding substituents, the experimental and theoretical evidence presented here suggests that $CH(SiMe_3)_2$ ligands are not particularly effective kinetic shields—these ligands clearly allow for the association of the reactive intermediates in the solid state. More specifically, for pnictinyl radical dimerization to take place it is necessary for the radicals to undergo a conformational change which, in turn, demands flexibility on the part of the ligands. In the process of bond formation the dimers **1** and **2** acquire a significant cache of potential energy that is manifested in a plethora of deformations. Ligands such as $CH(SiMe_3)_2$ can be considered to be the equivalent of molecular springs whose energy is of a magnitude capable of effecting chemical change. Such an understanding of the importance of ligand properties may allow for the rational design of substituents suitable, for example, for the long-term storage and spontaneous in situ generation of highly reactive species. Potential ligand candidates that should demonstrate this kind of behavior must be (a) somewhat flexible, and (b) capable of undergoing significant conformational change(s). Substituents that meet these requirements include e.g. PnR_2 (Pn = P, As, Sb) and ERR'_2 (E = Si, Ge, Sn; R′ = bulky ligand).

The generality of the foregoing interpretations is supported by the behavior of related systems that feature $CH(SiMe_3)_2$ ligands such as $(MR_2)_2$ (M = Ge, Sn).[8,9] These molecules dissociate to MR_2 carbenoids in solution and display analogous *syn,anti* to *syn,syn* conformational changes in the process.

Acknowledgment. We thank the Engineering and Physical Sciences Research Council, U.K. (EPSRC) for financial support of the Edinburgh Electron Diffraction Service (Grant GR/K44411) and for the Edinburgh ab initio facilities (Grant GR/K04194). We are also grateful both to the National Science Foundation (NSF) and the Robert A. Welch Foundation (UT-Austin) and EPSRC (Sussex) for funding. We also thank Dr. V. Typke of the University of Ulm for the variable-array version of the ASYM40[12] program, and the U.K. Computational Chemistry Facility (administrator: Department of Chemistry, King's College London, Strand, London WC2R 2LS, U.K.) for computing time.

Supporting Information Available: For the single-crystal structure determination, tables of crystal data and structure refinement, atomic coordinates, and anisotropic displacement parameters; for the gas-phase electron-diffraction study, experimental details, parameter and amplitude restraints, least-squares correlation matrices and the atomic coordinates for the final geometry; and for the ab initio study, theoretical geometrical parameters at the UHF/6-31G* and UHF/DZP levels (PDF); CIF data. This material is available free of charge via the Internet at http://pubs.acs.org.

JA010615B